Available online at www.sciencedirect.com
ScienceDirect
Ceramics International 36 (2010) 1529–1533
CERAMICS INTERNATIONAL
www.elsevier.com/locate/ceramint

Influence of Co content on the characterization and magnetic properties of magnetite

M.A. Ahmed [a,*], N. Okasha [b], S.I. El-Dek [a]

[a] *Materials Science Lab (1), Physics Department, Faculty of Science, Cairo University, Giza, Egypt*
[b] *Physics Department, Faculty of Girls, Ain Shams University, Cairo, Egypt*

Received 29 October 2009; received in revised form 29 December 2009; accepted 2 February 2010
Available online 9 March 2010

Abstract

Preparation of nanosized $Co_xFe_{3-x}O_4$; $0.05 \leq x \leq 0.20$ particles from metal nitrates solution through citrate–precursor method was performed. XRD pattern of all prepared systems showed single phase with cubic spinel structure. The crystallite size was determined from TEM and found to agree with that calculated from Sherrer's equation (60–76 nm) The magnetic constants such as molar magnetic susceptibility (χ_M), Curie temperature (T_C) and saturation magnetization (M_S) were measured and the results indicated that, at $x = 0.2$ the values of χ_M, M_S, remanent magnetization (M_r,) and coercive field (H_c) are 23 emu/g mol, 77.62 emu/g, 33.17 emu/g and 574.5 Oe, respectively.

Keywords: A. Nanopowder: chemical preparation; B. Electron microscopy; C. Magnetic properties; D. Spinel; Magnetite

1. Introduction

Magnetic nanoparticles are of great technological importance because of their use in magnetic fluid, information storage system, medical diagnosis and their interest in fundamental science, especially for addressing the fundamental relationships between magnetic properties and their crystal chemistry and structure [1,2].

Recently, several methods were used to synthesize highly crystalline and uniformly sized magnetic nanoparticles of cobalt ferrite [3–6]. Most of these methods cannot be applied to a large scale and economic production because they require expensive and toxic reagents, complicated synthetic steps, high reaction temperature and long reaction time.

Among many preparation techniques, citrate method stands out as an alternative and highly promising method of preparation. This method is quite simple, fast and inexpensive since it does not involve intermediate decomposition and do not need calcining steps. Moreover, it is easy to control the stoichiometry and crystallite size, which have important effect on the magnetic properties of the ferrite [1].

It is well known that, the bonding of two ferric ions and one ferrous ion with four ions of oxygen creates the unique mineral known as magnetite [7]. This mineral possesses strong magnetic properties and it is the only substance found in nature as a natural magnet [8].

Magnetite is an iron oxide of the spinel group of minerals [9,10] with the formula Fe_3O_4 (72.36% iron and 27.64% oxygen) [11]. This mineral crystallizes such that Fe^{3+} occupy the A sublattices in the tetrahedral sites and that the octahedral ones are filled in equal amounts of Fe^{3+} and Fe^{2+} ions (B sublattice).

Magnetite is one of the most studied transition metal oxides owing to its interesting magnetic and electrical properties. Due to its high magnetic and thermal properties, good electric conduction, and black color, it becomes a new type of materials promising in magnetic recording field [12–14]. It is also used in high recording density applications such as video and audio tape, instrument tapes, and flexible disks. It is needed to increase the coercivity of magnetite particles further.

Koseki et al. [15,16], studied the effects of co-substitution of Mn and Ni on the thermoelectric properties of sintered magnetite in $(Mn_yNi_{1-y})_x\,Fe_{3-x}O_4$; with $x = 0$–0.4 and $y = 0$–1. From these experiments, it was found that the thermoelectric power factor manifests a maximum near $y = 2/3$, where the

* Corresponding author.
E-mail address: moala47@hotmail.com (M.A. Ahmed).

0272-8842/$36.00
doi:10.1016/j.ceramint.2010.02.017

number of 3d electrons in magnetite is preserved by substitution.

Xiyun et al. [17] modified the as prepared magnetite by reaction with alkaline solution containing Co^{2+} and Fe^{2+} to obtain a cobalt ferrite layer on the surface of particles. They found that, the optimum conditions occur at cobalt content of 2.71% by weight and pH value of 12. Moreover, the formation of $CoFe_2O_4$ on the surface of the magnetite results in an increase of the coercivity (H_c = 45.60 kA/m, and the saturation magnetization M_s = 92 A m^2/kg).

Moreover, magnetite [18–23] has attracted much attention in the last few years due its excellent magnetic properties, and its use in biomedical applications especially with particle size of less than 10 nm where it exhibits superparamagnetic behavior.

The objective of this work is to prepare and characterize magnetic nanoparticles of Co doped magnetite using one-step citrate method without subsequent calcinations.

2. Experimental details

Nanocrystalline cobalt magnetite $Co_xFe_{3-x}O_4$ ($0.05 \leq x \leq 0.20$) was prepared using citrate method [24] with raw chemicals, Fe $(NO_3)_3{\cdot}9H_2O$, Co $(NO_3)_2{\cdot}6H_2O$ and citric acid, from British Drug House (BDH) 99.9% purity. Citrate complexes of the constituent metal ions were prepared by mixing metal nitrates and citric acid with a ratio (1:1) in triply distilled water. The individual metal–citrate complex solutions were mixed together with constant stirring to form the citrate–precursor mixture. Drops of ammonia solution were added to the precursor solution to maintain a pH value of 7. The sol was formed during stirring. Increasing the temperature of the hot plate and keeping constant stirring constantly, the water in the solution was evaporated and a viscous gel was formed. When keeping on heating, the gel is dried and burnt as being ignited to form loose powder. Differently from the reported previous work [24], a chelating agent such as ethylene glycol was not used, additionally the gel was not dried but it was forced to auto-combust in few minutes by keeping heating after gelation. This makes the process more simple, economic and fast for preparing large amounts of material.

A dried product in the form of uniformly colored gray fibers is obtained after 5 min from the sol formation.

The prepared powder was characterized by X- ray diffraction using a diffractometer model Proker D_8 with Cu Kα radiation (λ = 0.15418 nm) in a wide range of Bragg's angle (from 20° to 80°) at room temperature. The dc magnetic susceptibility (χ_M) of the investigated samples was measured using Faraday's method as a function of temperature and at different applied magnetic field intensities. The accuracy of measuring temperature in the magnetic susceptibility measurements was ±1 °C where the data were reproducible. The hysteresis and magnetization measurements were performed using vibrating sample magnetometer (VSM; 9600-1 LDJ, USA) with a maximum applied field of 15 kOe at room temperature.

3. Results and discussion

The structure of the as synthesized cobalt doped magnetite was identified by X-ray powder diffraction (Fig. 1a). The analysis of XRD pattern confirms the formation of single-phase spinel structure as indexed and compared with Fe_3O_4 (ICDD card no. 75-449, face centered cubic structure). Also the electron diffraction pattern, Fig. 2c agrees with the XRD results. XRD reflections are not too broad because 60–70 nm particles are not too fine or too small to reveal such expected broadening. The crystallite size is calculated from Scherrer's equation [25], $L = 0.89\lambda/\beta \cos\theta$; where β is the half peak width and λ is the wavelength of the radiation. Moreover, the agglomeration of the Co doped magnetite particles as seen from the TEM, Fig. 2a and b, could be a reasonable cause of the well-defined reflections where the particle size is relatively large. The dependence of the lattice parameter (a) on Co^{2+} content is shown in Fig. 1b. It reveals a decrease with increasing Co concentration due to smaller ionic radius of Co^{2+} ions (r_{Co} = 0.745 nm) which replaces Fe^{2+} (r_{Fe} = 0.078 nm) on octahedral sites. In other words, the decrease in *a* is due to the

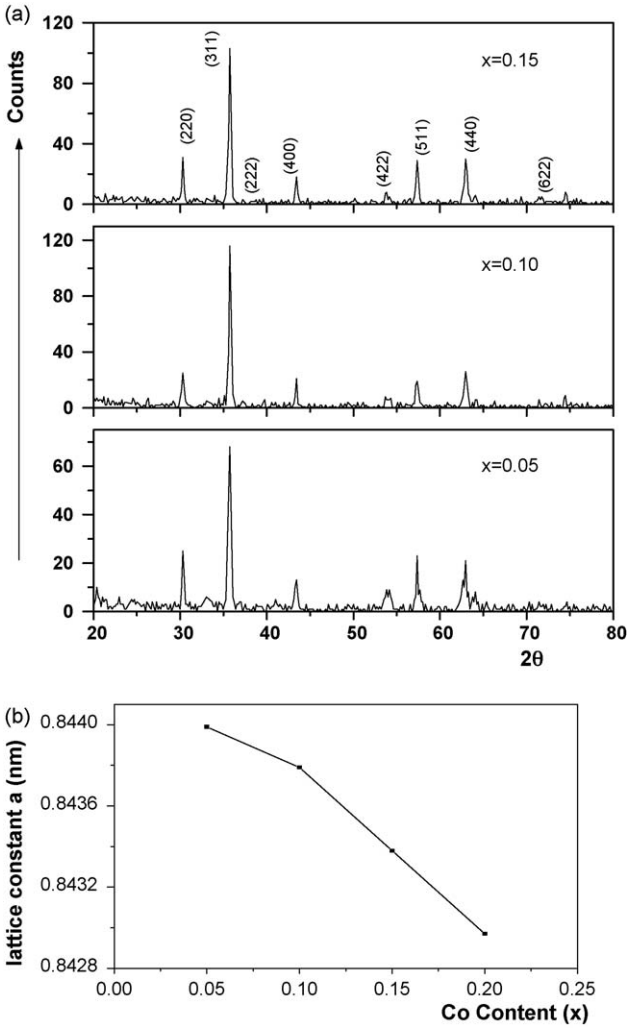

Fig. 1. (a) X-ray diffraction pattern of Co doped magnetite samples, (b) the change of lattice constant (a) as a function of Co content (*x*).

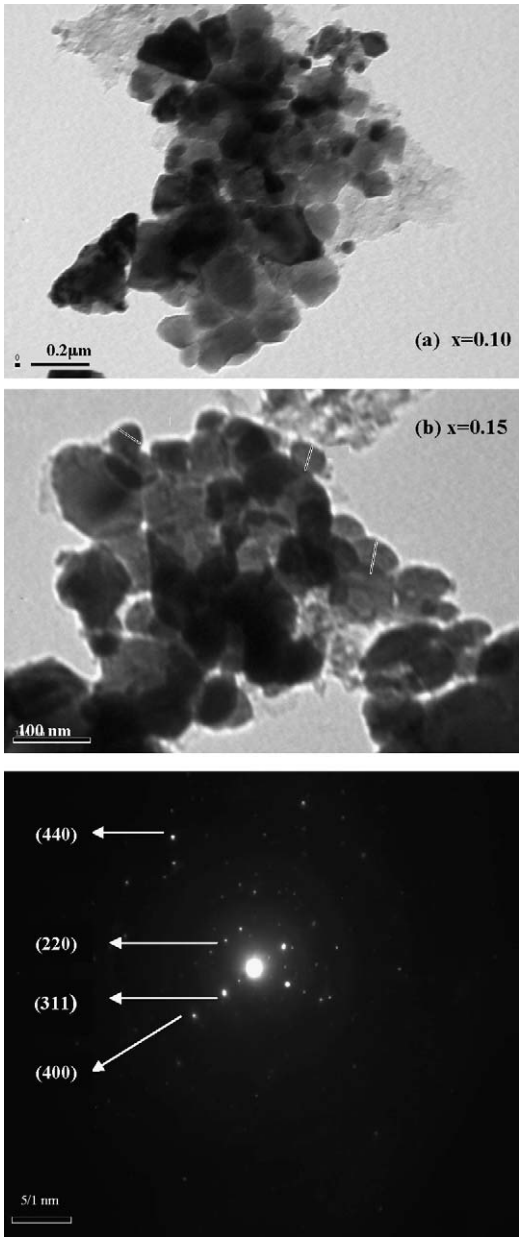

Fig. 2. TEM micrograph for the samples with (a) $x = 0.10$ and (b) $x = 0.15$. (c) Electron diffraction pattern for the sample with $x = 0.15$.

decrease of Fe^{2+} on octahedral sites where Co^{2+} ions are preferably located in the inverse spinel structure. With further increasing Co^{2+} content, one expect that it enters the A sites and this assumption is well supported by the results of the dependence of the saturation magnetization on Co content.

TEM micrograph of the samples $x = 0.10$ and 0.15 are illustrated in Fig. 2a and b. Most of the particles appear spherical in shape however some elongated particles are also present. More agglomerated than separated particles are present in the images. Agglomeration appears unavoidable due to the absence of surfactant. The average crystallite size calculated from the TEM is reported in Table 1 and match with that obtained from XRD data.

The average crystallite size (L) was calculated from X-ray line broadening using (3 1 1) peaks and Debye–Sherrer's equation [25] and the data are reported in Table 1. It is clear that, the crystallite size increases with increasing Co content except the sample with $x = 0.20$ which gives the smallest crystallite size. This could be explained on the basis of the statistical cation redistribution among the tetrahedral and octahedral sites. In other words, Co^{2+} replaces Fe^{2+} ions on the octahedral sites in magnetite as it is known to be an inverse spinel Fe^{3+} $[Fe^{2+}Fe^{3+}]O_4$ up to $x = 0.15$ and we expected that at $x \geq 0.2$ some Co^{2+} ions occupy the tetrahedral sites. At this concentration, the ratio of Fe^{2+}/Fe^{3+} is lowered to 0.4 which is considered to be critical.

Moreover, this behavior probably is due to the reaction condition, which favored the formation of new nuclei preventing further growth of particles when Co^{2+} ions increased. [26,27].

Fig. 3a–d illustrate the dependence of the dc molar magnetic susceptibility on the absolute temperature for as prepared samples $Co_xFe_{3-x}O_4$; $0.05 \leq x \leq 0.20$. The general trend of the data is nearly the same but with different values of both χ_M and Curie temperature (T_C) Table 1. The samples under investigation are ferrimagnetic from room temperature up to nearly the Curie point (T_C) of 800 K. The characteristic feature of the samples with $x \geq 0.05$ is the increase of the convex shape of the curves due to approaching the trend of Co ferrite. This behavior can be interpreted as because the thermal energy is not sufficient to give the chance to the spins to align in the magnetic field direction. When further increasing temperature, some of the spins are oriented towards the field direction but up to a certain temperature. The value of the anisotropy constant for Fe_3O_4 is -1.2×10^5 erg/cm^3 and for $CoFe_2O_4$ is $+3.2 \times 10^6$ erg/cm^3 [28] therefore; relatively high Curie temperature is achieved. The entropy increases with temperature destroying the magneto-crystalline anisotropy of the Co doped magnetite at the Curie point beyond which the samples behave as a typical paramagnet.

The cation distribution of the investigated samples is suggested to be Fe^{3+} $[Co_x{}^{2+}Fe_{1-x}{}^{2+}Fe^{3+}]O_4$, from this distribution and as it was clarified from XRD analysis, the

Table 1
Structural and magnetic parameters at room temperature for the samples $Co_xFe_{3-x}O_4$.

x	Crystallite size L (nm) from (3 1 1) plane	Average crystallite size L (nm)	Crystallite size L (nm) TEM	a (nm)	T_c (K)	H_c (Oe)	M_s (emu/g)	M_r (emu/g)
0.05	63	60	–	0.8439	805	250.9	52.98	9.40
0.10	72	68	60	0.8437	793	357.2	71.25	18.43
0.15	76	72	65	0.8433	783	467.5	72.22	25.73
0.20	60	56	–	0.8429	823	574.5	77.62	33.17

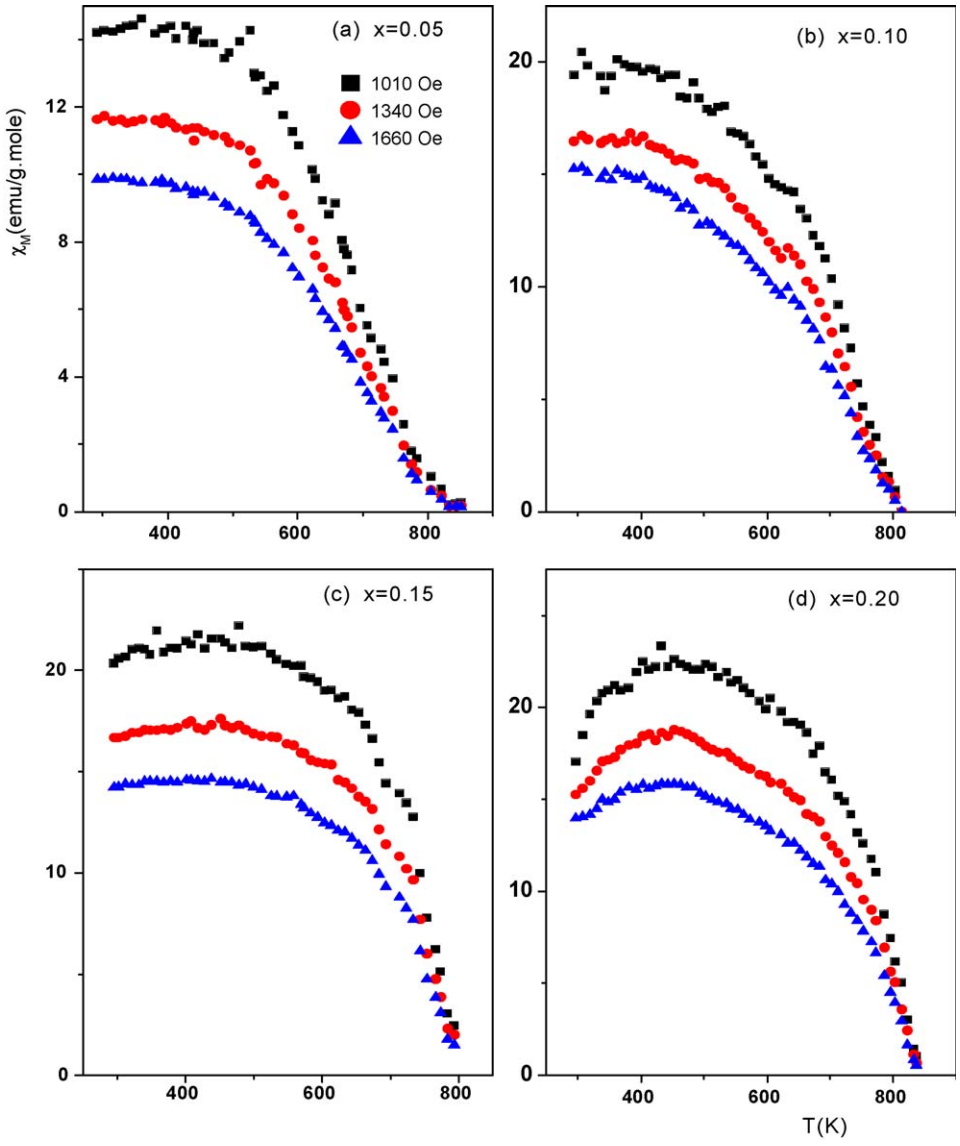

Fig. 3.

Co^{2+} ions replace some Fe^{2+} on octahedral sites [29]. With further increase in Co^{2+}, they enter the tetrahedral sites replacing some Fe^{3+} ions. This interpretation is quite supported by the decrease in the lattice parameter as discussed above as well as the increase in the saturation magnetization M_s (Fig. 4) as clarified from the hysteresis and reported in Table 1. The sample with $x = 0.2$ show an asymmetric hysteresis loop due to an effect known as the exchange bias effect. A simple model for explaining the exchange bias effect was proposed by Mieklejohn and Bean [30,31]. In a bilayer system of ferromagnetic (FM) and antiferromagnetic (AFM) layers, when the field is applied at temperature which is less than the Curie temperature of the FM layer and is above the Néel temperature of the AFM layer, the spins of the low-anisotropy FM material align with the applied field. When the temperature is lowered through the Neél temperature of the AFM layer its spins align with respect to each other and may couple with the FM spins depending up on the interfacial exchange coupling

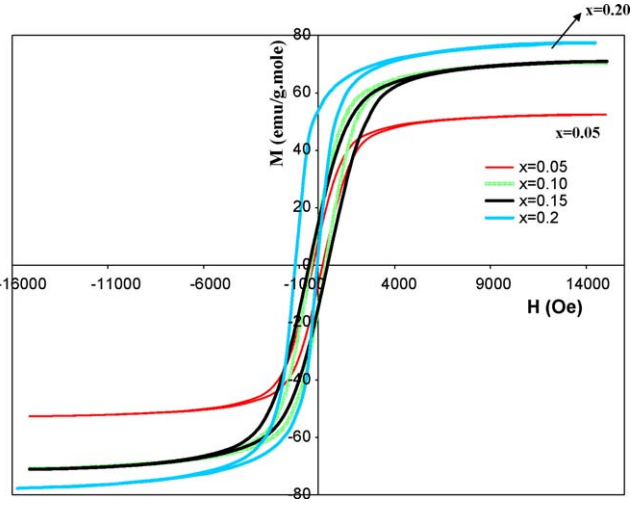

Fig. 4. Hysteresis loops of the investigated samples $Co_xFe_{3-x}O_4$; $0.05 \leq x \leq 0.20$.

between the two layers. This will generate a uniaxial anisotropy parallel to the cooling field direction. This is due to the large anisotropy of the AFM layer that prevents the AFM spin rotation and these in turn prevent the FM spin in turning away from the cooling direction.

The increase in M_S is directly related to the decrease in M_A due to the increase in Co^{2+} content on A site where, the total magnetization of $Co_xFe_{3-x}O_4$ is represented by: $M = M_B - M_A$; where M_A and M_B are the magnetization of A and B sublattices. With increasing Co content on A sites, M_A will be decreased, the result is the increase in the resultant magnetization. Due to replacement of Fe^{2+} by Co^{2+}, the crystallite size of the samples is increased. There are two ways to increase the coercivity of the ferrite particles either by improving the acicular form of the particles which increases the shape anisotropy or by increasing the magnetocrystalline anisotropy. Among the ferrites, $CoFe_2O_4$ has the largest positive anisotropy value due to the strong spin orbital coupling at Co^{2+} lattice sites. Co^{2+} doping enhances the magnetocrystallinity of the magnetite and hence enhances its coercivity as shown in Table 1. The increase in the coercive field with increasing crystallite size is an expected general trend [32,33]. Table 1 shows such behavior. The obtained values of M_s for our Co doped magnetite nanometric samples are higher than those obtained by Hong et al. [34] and Gnanaprakash et al. [35]. The values of the remanence magnetization (M_r) were found to increase with increasing Co content in the magnetite and higher than those obtained earlier [35].

The Curie temperature in ferrites is generally governed by the number of available Fe^{3+} ions, the separation between them and Fe^{3+}–O–Fe^{3+} bond angle and so the exchange interaction. For the investigated samples, the number of Fe^{3+} ions decreases on the expense of Co^{2+} ions. This results in a decrease in the value of T_C up to $x = 0.15$ and then increases again due to the cation redistribution which certainly led to a change in the A and B site radii. Accordingly, this alters the magnitude of the well-known antiferromagnetic superexchange interaction (AB). The values of T_C for our investigated Co^{2+} doped magnetite are slightly higher than that of $CoFe_2O_4$ (793 K) [35] and lower than that of Fe_3O_4 (860 K) [4].

4. Conclusions

Nanocrystalline magnetic particle of $Co_xFe_{3-x}O_4$ with $0.05 \leq x \leq 0.20$ were successfully prepared using the citrate method without subsequent heat treatment. The main advantage of the citrate method is that it is easy to prepare in one step, low cost, simple and gives fast and better results. The increase in the coercivity of the magnetite by Co^{2+} doping encourages us to recommend such magnetic nanoparticles in recording media applications.

References

[1] D.G. Gitchell, J. Magn. Reson. Imaging 7 (1997) 1.
[2] U. Hafeli, W. Schutt, J. Teller, M. Zborowski (Eds.), Scientific and Clinical Applications of Magnetic Carriers, Plenum, New York, 1997.
[3] N. Moumen, P. Veillet, M.P. Pileni, J. Magn. Magn. Mater. 149 (1995) 67.
[4] V. Pillai, D.O. Shah, J. Magn. Magn. Mater. 163 (1996) 243.
[5] Y. Ahn, E.J. Choi, S. Kim, H.N. Ok, Mater. Lett. 50 (1) (2001) 47.
[6] S.R. Ahmed, P. Kofinas, Mater. Res. Symp. Proc. 661 (2001) KK10.
[7] P.D. Franklin, S. Hill, The World's Most Magnificent Mineral Deposits, Excalibur Mineral Company, Franklin-Ogdensburg Mineralogical Society, New Jersey, 1995.
[8] H. Friedman, The Mineral Magnetite, Retrieved July 9, 2007, from the Mineral and Gemstone Kingdom, 2004.
[9] W.D. Nesse, Introduction to Mineralogy, Oxford University Press, New York, 2000.
[10] C. Klein, C.S. Hurlbut, Manual of Mineralogy, 21th ed., John Wiley & Sons, 1998.
[11] D. Barthelmy, Magnetite mineral data (2005) from mineralogy database web site http://webmineral.com/data/magnetite.shtml.
[12] H. Masacchika, W. Hiroyuki, M. Takeshi, Magnetic Particles and Process for Production, vol. 11, Japan EP0808801, 1997.
[13] G. Bate, J. Magn. Magn. Mater. 100 (1991) 413.
[14] N. Koji, K. Kouji, S. Seiji, Processes for producing Hydrated Iron Oxide and Ferromagnetic Iron Oxide, vol. 8, Japan EP0857693, 1998.
[15] Y. Zhu, Q. Wu, J. Nano Part. Res. 1 (1999) 393.
[16] N. Koseki, Y. Oikawa, C. Kim, H. Ozaki, Y. Nakada, Proc. of the 22nd International Conference on Thermoelectric, 2003.
[17] Y. Xiyun, G. Zhuqing, L. Feng Liang, H. Jian, Trans. Nanoferrous Met. Soc. China 15 (2005) 103.
[18] J.H. Xia, H. Shen, B.F. Shu, W. Zhang, Mat. Res. Bull. 43 (8–9) (2008) 2213.
[19] J. Mürbe, A. Rechtenbach, J. Töpfer, Mater. Chem. Phys. 110 (2–3) (2008) 426.
[20] P.C. Fannin, C.N. Marin, J. Magn. Magn. Mater. 320 (16) (2008) 2106.
[21] K. Nishio, Y. Masaike, M. Ikeda, H. Narimatsu, N. Gokon, S. Tsubouchi, M. Hatakeyama, S. Sakamoto, N. Hanyu, A. Sandhu, H. Kawaguchi, M. Abe, H. Handa, Colloids Surf B: Biointerfaces 64 (2) (2008) 162.
[22] T. Ozkaya, M.S. Toprak, A. Baykal, H. Kavas, Y. Köseoğlu, B. Aktaş, J. Alloys Compd. 462 (2008) 209.
[23] S. Mondini, S. Cenedese, G. Marinoni, G. Molteni, N. Santo, C.L. Bianchi, A. Ponti, J. Colloid Interface Sci. 322 (1) (2008) 173.
[24] A. Thakur, M. Singh, Ceram. Int. 29 (2003) 505.
[25] B.D. Cullity, Elements of X-Ray Diffraction, 2nd ed., Addison-Wesley Publ. Company, 1978.
[26] T. Orth, M. Moller, J. Pelzl, et al. J. Magn. Magn. Mater. 145 (1995) 243.
[27] Y. Wei, J. Xin, X. Jin, Fine Chem. 14 (1) (1997) 29.
[28] B.G. Toksha, Sagar E. Shirsath, S.M. Patange, K.M. Jadhav, Solid State Commun. 147 (2008) 479.
[29] M.A. Ahmed, S.F. Mansour, S.I. El- Dek, AIP Conf. Proc. 888 (2007) 122.
[30] W.H. Meiklejohn, C.P. Bean, Phys. Rev. 105 (1957) 904.
[31] W.H. Meiklejohn, C.P. Bean, Phys. Rev. 102 (1956) 1413.
[32] B.X. Gu, Appl. Phys. Lett. 82 (2003) 3707.
[33] Y.W. Dou, Ferrites, Jiangsu Technology Publishing Company, Nanjing, 1996, pp. 62–69 (in Chinese).
[34] R. Hong, J. Li, J. Wang, H. Li, China Particuol. 5 (2007) 186.
[35] G. Gnanaprakash, S. Mahadevan, T. Jayakumar, P. Kalyanasundaram, John Philip, Baldev Raj, Mater. Chem. Phys. 103 (2007) 168.